Simultaneous measurement of NO and NO_2 by dual-channel cavity ring down spectroscopy technique

Renzhi Hu (1) †*, Zhiyan Li (1, 2) †, Pinhua Xie (1, 3, 5) *, Hao Chen (1), Xiaoyan Liu (4), Shuaixi Liang (1, 2), Dan Wang (6), Fengyang Wang (1), Yihui Wang (1, 3), Chuan Lin (1), Jianguo Liu (1, 3, 5), Wenqing Liu (1, 3, 5)

(1) Key Lab. of Environmental Optics and Technology , Anhui Institute of Optics and Fine Mechanics, Chinese Academy of Sciences, Hefei 230031,China.

(2) Science Island Branch of Graduate School, University of Science and Technology of China. Hefei 230026, China.

(3) School of Environmental Science and Optoelectronic Technology, University of Science and Technology of China, Hefei 230027, China.

(4) College of Pharmacy, Anhui Medical University, 81 Meishan Road, Hefei 230032, China.

(5) CAS Center for Excellence in Regional Atmospheric Environment, Institute of Urban Environment, Chinese Academy of Sciences, Xiamen, 361000, Fujian, China.

(6) School of Mathematics and Physics, Anhui University of Technology, Ma an Shan 243032, China.

†These authors contributed equally to this work.

*e-mail: rzhu@aiofm.ac.cn, phxie@aiofm.ac.cn

Key words: NO_x; CRDS; CEAS; CL

Abstract

Nitric oxide (NO) and nitrogen dioxide (NO_2) are relevant to air quality due to their roles in tropospheric ozone (O_3) production. In China, NOx emissions are very high and NOx emissions exhausted from on-road vehicles make up 20% of total NOx emissions. In order to detect the NO and NO_2 emissions on road, a dual-channel cavity ring down spectroscopy (CRDS) system for NO_2 and NO detection has been developed. In the system, NO is converted to NO_2 by its reaction with excess O_3 in NO_x channel, such that NO can be determined through the difference between two channels. The detection limits of NO_2 and NO_x for the system are estimated to be about 0.030 ppb (1σ, 1 s) and 0.040 ppb (1σ, 1 s), respectively. Considering the error sources of NO_2 absorption cross section and R_L determination, the total uncertainty of NO_2 measurements is about 5%. The performance of the system was validated against a chemiluminescence (CL) analyzer (42i, Thermo Scientific, Inc.) by measuring the NO_2 standard mixtures. The measurement results of NO_2 showed a linear correction factor (R^2) of 0.99 in a slope of 1.031 ±0.006, with an offset of (-0.940 ±0.323) ppb. An intercomparison between the system and a cavity-enhanced absorption spectroscopy (CEAS) instrument was also conducted separately for NO_2 measurement in ambient environment. Least-squares analysis showed that the slope and intercept of the regression line are 1.042 ± 0.002 and (-0.393 ± 0.040) ppb, respectively, with a linear correlation factor of $R^2 = 0.99$. Another intercomparison conducted between the system and the CL analyzer for NO detection also showed a good agreement within their uncertainties, with an absolute shift of (0.352 ± 0.013) ppb, a slope of 0.957 ±0.007 and a correlation coefficient of $R^2 = 0.99$. The system was deployed on the measurements of on-road vehicle emission plumes in Hefei, and the different emission characteristics were observed in the different areas of the city. The successful deployment of the system has demonstrated that the instrument can provide a new method for retrieving fast variations of NO and

NO₂ plumes.

1. Introduction

In recent years, with the improvement of people's living standard, more and more attention is given

45 to the improvement of the living environment. Among which, the management of environmental pollution has gradually become one of the focus issues, and it is believed that the detection of pollutants is prerequisite for environmental governance. As one of the main air pollutants, NO_x (NO_x= NO+NO_2) is well known as one byproduct of organic decay, the emission from natural forest fires, as well as the main anthropogenic emission from both stationary sources (electric power generation using fossil fuels)

50 (Jaramillo and Muller, 2016) and mobile sources (motor vehicles and catalytic converters of most cars) (Carslaw, 2005). NO_x can determine the tropospheric O_3 levels which can lead to the formation of photochemical "smog". Furthermore, NO_x is also known as the precursor of nitric acid (Brown et al., 2004). In addition, NO_x can do harm to the human body and animals by damaging the respiratory system and leading to pulmonary edema (Yang and Omaye, 2009). Moreover, it is believed that accurate NO_2

55 measurement plays a key role in accurate measurement of other species, such as organic nitrate (Thieser et al., 2016; Paul et al., 2009; Day et al., 2002) and RO_2 radicals (Chen et al., 2016).

During the last few years, many direct and indirect techniques for monitoring NO_2 have been established, such as chemiluminescence (CL) detection (Yuba et al., 2010; Sadanaga et al., 2008; Fahey et al., 1985), differential optical absorption spectroscopy (DOAS) (Platt et al., 1984;R. McLaren, 2010),

60 tunable diode laser absorption spectroscopy (TDLAS) (Li et al., 2004), cavity ring-down spectroscopy (CRDS) (Castellanos et al., 2009; Fuchs et al., 2009; Osthoff et al., 2006; Fuchs et al., 2010; Brent et al., 2013 ; Hu et al.,2015), cavity enhanced absorption spectroscopy (CEAS) (Wu et al., 2009; Gherman et al., 2008; Kasyutich et al., 2006; Wada and Orr-Ewing, 2005), cavity attenuated phase shift spectroscopy (CAPS) (Kebabian et al., 2008), laser-induced fluorescence (LIF) (Taketani et al., 2007; Matsumi et al.,

65 2010; Sadanaga et al., 2014; Matsumoto et al., 2001) measurement, long path absorption photometer` (LOPAP) (Villena et al., 2011) and gas based sensors (Novikov et al., 2016), with CL being the most widely used for in situ ambient sampling. CL can achieve direct measurement of NO and indirect measurement of NO_2. The method is based on the reaction between NO and O_3, which can form an electronically excited molecule of NO_2*. When NO_2* reaches the ground state, it emits fluorescence

70 which is proportional to the initial NO concentration. While NO_2 is measured indirectly by conversion to NO firstly through heated (300 ℃ to 350 ℃) molybdenum (Mo) surfaces (Ridley and Howlett, 1974) or photolytic NO_2 converters like Xenon lamps or UV emitting diodes at specific wavelength (320 nm-400 nm). The CL instruments have typical NO_2 detection limits of 50 ppt /1 min (1σ) (Wang et al., 2001). By contrast, CRDS, CEAS, CAPS and TDLAS, generally relying on scanning a light source through a

75 range of frequencies of interest, are all direct absorption techniques. It has been demonstrated that these optical methods can achieve a high detection sensitivity and the detection limit is several ppt level with several seconds time resolution (Li et al., 2004; Wild et al., 2014; Gherman et al., 2008; Kebabian et al., 2008). Among these techniques, CRDS has become a promising technique for ambient NO_2 detection due to its advantages of high time resolution, low detection limit as well as portability, in which pulsed

80 (Fuchs et al., 2009) or continuous-wave (cw) lasers(Wada and Orr-Ewing, 2005) were utilized. Wada et al. (Wada and Orr-Ewing, 2005) demonstrated a cw diode CRDS system operating at 410 nm for the retrieval of NO_2 mixing ratios in ambient air with a detection limit of 0.1 ppb in 50 s at atmospheric pressure. Osthoff et al. (Osthoff et al., 2006) constructed a pulsed cavity ring-down spectrometer where a pulsed (20–100 Hz, up to 25 mJ) frequency-doubled Nd:YAG laser was used for the simultaneous

85 measurements of NO_2, nitrate radical (NO_3), and dinitrogen pentoxide (N_2O_5) in the atmosphere, and the detection limit of 40 ppt (1σ) for 1 s data was achieved for NO_2 with an uncertainty within $\pm 4\%$ under laboratory conditions. Fuchs (Fuchs et al., 2009) used a simple, lightweight, low power, and commercially available Fabry-Perot (FP) diode laser with a center wavelength of 403.96 nm as a light source to detect NO and NO_2 in two separate channels. The limit of detection is 22 ppt (2σ precision) for

90 NO_2 at 1 s time resolution. Karpf (Karpf et al., 2016) used a high-power, multimode Fabry Perot (FP) diode laser with a broad wavelength range ($\Delta\lambda_{laser} \sim 0.6$ nm) to excite a large number of cavity modes, thereby reducing the susceptibility of the detector to vibration and making it well suited for field deployment. A sensitivity of 38 ppt was achieved using an integration time of 128 ms for single-shot detection in their work. To evaluate the uncertainty and the accuracy of the aforementioned individual

95 instruments, a number of intercomparison studies have been carried out (Xu et al., 2013; Dunlea et al., 2007; Villena et al., 2012). The comparison results show that the method based on Mo converters can be affected by significant interferences such as N_2O_5, HONO, HNO_3, PAN, etc. Whereas the method based on optical absorption is relatively immune to interferences. Therefore, direct techniques are considered to be more reliable methods than the CL method for the measurement NO_2 and have been adopted

100 gradually in field experiments (Ayres et al., 2015; Wagner et al., 2013; Sobanski et al., 2016).

In addition to the direct measurement of NO with the CL method, NO concentrations can also be measured directly based on their absorption feature at 1,585.282 cm^{-1}. For example, a tunable infrared laser differential absorption spectroscopy (TILDAS) instrument based on a DFB laser emitting sequentially at 1,600 cm^{-1} and 1,900 cm^{-1} have been used by Jagerska et al for the measurement of NO

105 and NO_2 (Jagerska et al., 2015), where an astigmatic multi-pass Herriott cell (Herndon et al., 2004) and a dual-wavelength spectrometer are utilized. The 1 s precision for NO measurement of the TILDAS instrument was 550 ppt, whereas that for the field experiments was 1.5 ppb. Compared with the CL method, it seems that this technique may suffer from low detection sensitivity. Given the rapid changes of nighttime oxidation, i.e., NO_3 radical, the rapid changes of its precursors, NO and NO_2 is thus a

110 prerequisite for developing a nighttime atmospheric chemistry model. To achieve high sensitivity and high resolution, conversion to NO_2 by adding excess O_3 may be one of the best methods for NO detection(Fuchs et al., 2009; Wild et al., 2014).

The developments of different technologies provide the potential for NOx measurements on different platforms such as ground sites, vehicles as well as aircrafts (Yamamoto et al., 2011; Wagner et

115 al., 2011; Castellanos et al., 2009). Due to the rapid economic growth in 2000-2010, China has become the second largest economy in the world. With the rapid growth of energy consumption, NOx emissions are increasing. Motor vehicles are one of the major sources for NOx, especially in urban areas (Westerdahl, 2008). Exhaust from on-road vehicles makes up 20% of total NOx emissions in China (Shi et al., 2014). So various methods have been used to measure the vehicle emissions to assess exposure to

120 air pollutant and specifical impacts due to traffic-related emissions (Vogt et al., 2003; Carslaw and Beevers, 2004; Herndon et al., 2005; Lal et al., 2005; Burgard et al., 2006b; Hueglin et al., 2006; Burgard et al., 2006a; Wild et al., 2017). However, the measurements were usually carried out at several fixed locations in large cities, which is not adequate to show the large scale patterns of the cities. Hence, a direct on-road mobile instrument is needed to obtain the spatial and temporal variations of NOx pollutants.

125 In this work, a dual-channel CRDS system has been developed based on the chemical conversion of NO to NO_2, which realizes the simultaneous measurement of NO_2 and NO_x. In one channel, only ambient NO_2 is measured. In another channel, the sum of ambient NO_2 and the converted NO_2 from ambient NO is determined to provide a direct measurement of NO_x. Then the difference of the two

channels provides a direct measurement of NO. To assess the accuracy of the dual-channel CRDS instrument, contrast measurements and comparison were conducted between the dual-channel CRDS instrument with the other different instruments. In addition, the instrument was deployed in the measurement of on-road vehicle emission plumes in the city of Hefei, China on December 17, 2018 and February 25, 2019. The main advantages of this instrument compared with CL instruments are also discussed as well as its potential ability for trace measurements.

2. Setup of the instrument

Due to its high detection sensitivity, cavity ring-down spectroscopy has been applied to measurement NO_3 radical and N_2O_5 in our group (Wang et al., 2015; Li et al., 2018; Li et al., 2018). In this work, the technique was applied to measure NO_2 and NO simultaneously. A schematic diagram of the dual-channel CRDS system developed in the present work is shown in Fig. 1. The instrument mainly consists of two identical CRDS systems for NO_2 and NO_x detection, gas handling system, NO convertor and activated carbon device for NO_x removing.

2.1. CRDS systems

A blue diode laser is used as the light source and the wavelength of the laser is monitored in real time by a spectrometer. The output of the diode laser, with a center wavelength at 403.64 nm and a line width of 0.5 nm, is directly modulated by a square wave signal (on/off) at a repetition of 2 kHz with a duty cycle of 50%. And generally the output power is about 60 mW. The laser beam first passes through an isolator to prevent the reflected light back into the laser cavity, then is divided into two approximately equal beams after a 50/50 beam splitter and enters into two identical cavities separately. Each optical cavity is made of an aluminum tube with an inner diameter of 9.4 cm, which is fixed rigidly by a separate frame. Two high reflectivity mirrors are held in stable, adjustable mounts. The distance between the two highly reflective mirrors (LGR, 1 in. diameter, 1 m radius of curvature) in each channel is 75 cm, which corresponds to the ring-down time constants of 22.90 μs and 24.12 μs for NO_x and NO_2 cavities in zero air. The light emitted through the back mirror of the cavity passes through a narrowband filter to filter stray light, and then is directed into a PMT. The signal is amplified firstly, then acquired with digital acquisition card (NI USB-6361, 16-bit, 2.0 Ms/s). The sampling frequency for each digital acquisition card is 1 MHz. During a continuous 1.0 s data acquisition period , 2000 decay traces are transferred to the PC using a single transfer command and averaged to get a fitted decay trace at a laser modulation rate of 2 KHz. NO_2 concentration can be calculated according to Equ.1 from the ring-down times, τ and τ_0, the ring-down times when the NO_2 is in the presence and absence of the cavity, respectively; the NO_2 absorption cross section, R_L is the ratio of the total cavity length to the length over which the absorber is present in the cavity, and c the speed of the light.

$$[NO_2] = \frac{R_L}{c\,\sigma_{NO_2}} \left(\frac{1}{\tau} - \frac{1}{\tau_0}\right) \tag{1}$$

2.2. NO convertor

NO is measured by its conversion to NO_2 in the presence of excess O_3. The principle is based on the following chemical equation (Sander et al., 2006).

$$NO + O_3 \rightarrow NO_2 + O_2 \quad k_1 \tag{R1}$$

where $k_1 = 3.0 \times 10^{-12} \exp(-1310/T)$ cm^3 $molec^{-1}$ s^{-1}. Ozone is produced from O_2 photolysis at 185 nm by flowing 100 sccm of sampling air over a low pressure discharge mercury lamp. The mercury lamp is

inset into a quartz glass tube with a length of 50 mm and an inner diameter of 10mm. The flow rate passing through the mercury lamp was controlled by a MFC and the resulting mixing ratio of O_3 was detected by an O_3 analyzer (49i, Thermo Scientific). The O_3 concentration is approximately 11.2 ppm after mixing with the sampled air. A Teflon tubing (length 1 m, i.d. 3.8mm) serves as a reactor for the NO conversion.

2.3. Activated carbon device

Accurate measurement of the ring down time, τ_0, when there is no any absorber in the cavity, is pivotal for accurately retrieving the absorber concentration in a practical measurement as well as for checking the cleanliness of the cavity mirrors. Usually zero air or chemical scrubber is used to acquire zeros (Wada and Orr-Ewing, 2005). In our system, zeros are obtained by passing sampled air through an activated carbon filled tube with a length of 26.0 cm and an outer diameter of 6.0 cm. The τ_0 is measured for 60 s every 10–16 min. It is found that this frequency of zero measurements is sufficient to track drifts in the zero ring-down time constant measurement, i.e. the fluctuation of τ_0 is less than 0.1% for 15 min intervals.

2.4. Gas handling system

The gas handling system of the instrument consists of a sampling module and a purge flow. The sampled air initially flows through a filter device, where a filtering membrane (1 μm pore size) is loaded to prevent light-scattering aerosols from entering the cavity. And subsequently it will pass through the activated carbon device to provide the background measurement or enter the PFA tube directly just depending on whether the three-way solenoid valve is open or closed. After the PFA tube, the air flowis divided into three lines. The first flow (100 sccm) is introduced into a quartz flow tube equipped with a mercury pen-ray lamp (Oriel 6035) to generate O_3 by air photolysis as aforementioned, then it will be merged with the second sampling flow (900 sccm) and pulled into the NO_x cavity. The third one with a flow rate of 1 slm is directed into the NO_2 cavity. All the system is pumped by a rotary pump (K86KNE) and the flow rates of the different lines are controlled by mass flow controllers separately. To prevent the degradation of the mirror reflectivity, each mirror is continuously flushed with high-purity nitrogen at a rate of 25 ml min^{-1} to avoid the potential pollution from the sample flow.

3. Results and discussion

3.1 Determination of Absorption Cross Sections

To retrieve the gas concentration, it is prerequisite to determine the effective absorption cross section at peak absorption of the laser. The output waveforms of the laser, with a center wavelength of 403.64 nm and full width at half-maximum of 0.5 nm, was monitored by a spectrometer (QEPB0828) (red line shown in Fig. 2). The center wavelength selected can cover the strong absorption of NO_2 and avoid the interference from other species, such as H_2O (pink line in Fig. 2). The effective absorption cross section was determined to be 5.63×10^{-19} cm^2/molecule by convoluting the NO_2 absorption cross section with the laser spectrum (blue line in Fig. 2) using voigt profile (Voigt et al., 2002). It is well known that a shift in the laser center wavelength would result in a change of the effective NO_2 cross-section, so the laser output was monitored as the index of the day-to-day variability of the laser center wavelength. It was shown that the variability is less than 1% during the experiment few days. The largest uncertainty of the absorption cross section is about 3% according to voigt (Voigt et al., 2002).

3.2 The retrieval of R_L

Due to the purge gas to the mirrors, the R_L value cannot be simply determined by the ratio of the distance between two mirrors to that between the inlet and outlet. The R_L value of the system was determined from the absorption measurement of various concentrations of NO_2 ranging from 20 ppb to 70 ppb with or without purge flow. The ratio of the two extinction measurements yielded a R_L value, which is independent of the cross section and the concentration of NO_2. The R_L value is determined to be 1.10 ± 0.03 for both the NO_x and NO_2 channels.

3.3 The retrieval of τ_0

In order to accurately determine the concentrations of trace gas by CRDS, it is very important to confirm background cavity loss measurements of τ_0 when the target gases are not inside the cavity. Several alternative background measurement methods have been reported, where various kinds of air were used as background gas, such as zero air, a mixture of oxygen and nitrogen, chemically scrubbed laboratory air (using hydroxyapatite), and laboratory air sampled through the stainless steel tubing coil (Wada and Orr-Ewing, 2005). In our instrument, an activated carbon device was used for background measurement. The ring down times when the sampled air pass through the activated carbon device were determined to be 24.12 ± 0.01 μs and 22.90 ± 0.01 μs in two cavities, respectively. These values are close to those of measurements of zero air at the same sample rate for a 15 min period.

Two representative ring-down signals corresponding to with and without NO_2 in the cavity for the CRDS system are shown in Fig. 3. And the fitted ring down time were 24.12 μs and 20.30 μs respectively, so that the NO_2 concentration is determined as 20.28 ppb using the constants determined above.

3.4 Detection limit and measurement accuracy of two cavities.

The measurement precision of the dual-channel CRDS instrument for NO_2 and NO_x detection was investigated with time series measurement of zero air (Fig. 4). The acquisition time for the spectral data was 1.0 s with an average of 2000 spectra. In order to analyze the stability of the instrument, the Allan variance had been calculated for the intensity measurements. For the two channels, the 1σ detection limits were 30 ppt and 40 ppt (1s) for the NO_2 and NO_x channels, respectively. The minima in the Allan plots indicated that the optimum average times for optimum detection performance (right panel of Fig. 4) is about 30 s. With 30 s integration time, the 1σ detection limits were 16 ppt and 14 ppt for the NO_2 and NO_x channels, respectively.

The minimum detection can be written as follows:

$$[A]_{min} = \frac{\sqrt{2}R_L}{c\sigma}\left(\frac{\Delta\tau_0}{\tau_0^2}\right) \tag{2}$$

For continuous zero NO_2 measurements, the $\Delta\tau_0$ was 0.008 μs in both NO_x and NO_2 channels and τ_0 was 22.90 μs and 24.12 μs in NO_x and NO_2 channels, respectively for 1 s averaging. Given the R_L value to be 1.10 and σ to be 5.63×10^{-19} molecule/cm^2, the 1σ minimum detection limits for the NO_x and NO_2 channels were determined as 39 ppt and 35 ppt respectively at an integration time of 1 s, which are close to the Allan variance analysis described above.

The total uncertainty of NO_2 measurement by CRDS is expected to be from the uncertainties on the measurement of R_L and NO_2 absorption cross section. The uncertainty in R_L was determined to be less than 3%, and the uncertainty in the NO_2 absorption cross-section was about 4%, so the total uncertainty of NO_2 measurement was estimated to be 5% for the system in this work.

Compared with the existing field measurement techniques for NO_2 measurements, it seems that the

250   minimum detection and uncertainty of this instrument is superior to the other methods (see Table 1).

3.5 NO Conversion Efficiency

The main influence factor on the NO conversion efficiency is the flow rate passing through the mercury pen-ray lamp as it can determine the generated O_3 concentration. The mixing ratio of O_3 in the NO_x channel line changing with the flow rate that passes through the mercury pen-ray lamp was
255   investigated and the result is shown in Fig. 5. As a result, the bypass flow passing through the Hg lamp was determined to be 100 sccm. Under this flow rate, when the residence time of O_3 in the cavity is 1s and the ambient NO_2 concentration is 50 ppb, NO conversion efficiency with different NO concentrations (10-1000 ppb) was simulated and NO conversion efficiency in the range of experimental concentrations is larger than 98% .

260   Because the cross section of O_3 is about four orders of magnitude smaller than that of NO_2 at the center wavelength of the laser, the absorption of O_3 generated by mercury photolysis is negligible. According to Fuchs (Fuchs et al., 2009), under conditions when NO is rich, further oxidation of NO_2 to NO_3 and N_2O_5 has only a slight effect on NO_x measurement, which means that the correction of the NO_x measurement can be neglected. However, under conditions when NO is absent, the loss of NO_2 due to
265   oxidation by high concentration of ozone is indeed one of the main factors that attributes to the errors in the NO_x channel. The reaction equation is expressed as follows:

$$NO_2+O_3 \rightarrow NO_3+O_2 \qquad k_2 \qquad\qquad (R2)$$

$$NO_3+NO_2 \leftrightarrow N_2O_5 \qquad k_{eq} \qquad\qquad (R3)$$

where k_2 = 1.2×10^{-13} exp $(-2450/T)$ cm^3 molec^{-1} s^{-1} (T=298K, k_2 = 3.2×10^{-17} cm^3 molec^{-1} s^{-1})(Sander et
270   al., 2006), k_{eq} = $(5.1 \pm 0.8) \times 10^{-27}$ exp $(10871/T)$ cm^3 molec^{-1} s^{-1} (T=298K, k_{eq} = 3.5×10^{-11} cm^3 molec^{-1} s^{-1}) (Osthoff et al., 2007). The loss rate will increase with the increase of the $NO_2 + O_3$ reaction rate constant when temperature in the cavity increases. Moreover, the loss rate is also sensitive to the NO_2 mixing ratio. Diluted NO_2 standard mixture was introduced into the two channels to characterize the effect of high concentration ozone on NO_2 measurement. The NO_2 concentrations in the two channels and their
275   correlation are shown in Fig. 6. The interference of O_3 in NO_x channel when NO is absent can be neglected. The discrepancy between two different channels maybe result from the systematic errors in two different channels and can be corrected with the coefficient obtained from Fig. 6 (b).

4. Field applications

4.1 Contrast measurement of standard mixtures of NO and NO_2.

280   The comparisons of NO_2 measurements between CRDS and NO_x analyzer have been carried out on NO_2 standard mixtures. Different mixing ratios of NO_2 were obtained by gas phase titration of NO with excess O_3 generated by an ozone generator (OC500). The 10.3 ppm NO standard mixture was initially diluted by N_2 and subsequently oxidized by O_3. The amount of NO_2 generated from excess ozone can be calculated from the known initial concentration of NO. The generated pure NO_2 standards in clean air
285   were in the concentration range of 20-70 ppb. The CL analyzer used for comparison in this laboratory experiment was separately calibrated and the linearity of this instrument was checked using a mixture containing NO. Fig. 7 (a) shows the concentrations of the standard NO_2 in the laboratory measured by

CRDS and a commercial CL analyzer (42i, Thermo Scientific, Inc., 0.4 ppb (1σ) detection limit) simultaneously. A correlation analysis between the data from the two instruments was carried out. The fitting results shown in Fig. 7(b) indicate that $NO_{2\,(CRDS)} = NO_{2\,(CL\,analyzer)} \times 1.031 - 0.940$, with a linear correlation factor (R^2) of 0.99. The results in Fig. 7 (a) also indicate that CRDS instrument can capture the NO_2 variation more rapidly than CL analyzer.

4.2 Ground-based measurements of NO_2 and NO.

To verify its performance and applicability, the dual-channel CRDS instrument was further compared with a CEAS instrument (Duan et al., 2018) on ground-based measurement of NO_2 during the period from November 3 to 5, 2017 in the western suburb area of Hefei, Anhui, China. The reason why CEAS instrument not the CL analyzer was selected for NO_2 intercomparison is that for CL analyzer, NO_2 must be converted to NO first and then can be detected, which expose the analyzer to chemical interferences, while for CEAS instrument, NO_2 can be detected directly. Measurement precisions (1σ) for NO_2 is about 170 ppt in 30 s. The time resolution of CRDS and CEAS instruments are 1s and 1min respectively. The CRDS and the CEAS instruments were set up on the sixth floor of the building in Anhui Institute optic and Fine mechanics. The area lies to the northeast of the Dongpu reservoir and is about 1.5 km far from the reservoir. The northwest of the area is surrounded by a forest. The significant NO_2 pollution during the measurement was found to be the emission of the cars along the road (100 m radius). The air originated from the sector between the South and East (5 km) may bring the anthropogenic emission to the site. Ambient air was introduced into the instruments through a 6 mm outer diameter Teflon tube. The data for comparison were averaged to 1min. Fig. 8 (a) shows the temporal variations of NO_2 concentrations measured by the CEAS and the CRDS instruments respectively. It was found that the nighttime NO_2 was in the range of 3 ppb to 35 ppb. Generally, the NO_2 concentrations and variations measured by the CRDS instrument show good consistency with those measured by the CEAS instrument, and the slope and intercept of the regression line from the least-squares analysis are 1.042 ± 0.002 and (-0.393 ± 0.040) ppb, respectively as shown in Fig. 8(b). However, the results revealed a discrepancy when rapid NO_2 variations appeared. We attribute this discrepancy to the slight difference between the two inlets of the instruments when large NO_2 was rapidly emitted into the atmosphere. In general, the CRDS instrument has substantive advantages for retrieving rapid variations of NO_2 plums due to its high time resolution and high sensitivity.

The comparison of NO concentrations measured by the dual-channel CRDS instrument and CL analyzer was conducted under a variety of sampling conditions for a total of seven days at the site described previously. Both instruments were attached to the same air sample inlet. The data sets from the CRDS instrument and CL analyzer were highly correlated over wide concentration ranges of NO (see Fig. 9 (a)). Fig. 9 (b) shows the relationship between NO concentrations observed by the CRDS and CL methods. The slope and intercept of the regression line were 0.959 ± 0.007 and 0.352 ± 0.013 ppb. The correlation coefficient is $R^2=0.99$. As CL method is believed to be a reliable way for NO measurement, the reliability of the dual-channel CRDS instrument were validated for the measurement of NO.

4.3 On-road measurements of vehicle NO_2/NOx emission.

In order to retrieval the vehicle emissions on road, field measurements were performed in Hefei from 15:00 to 16:00 CST on 17 December 2018. The CRDS instrument was powered by a lithium battery, and ambient air was pumped into the system though an inlet fixed on the roof of the car. The vehicle speed is about 50 km/h. In order to get the discrepancy of vehicle emissions in urban and suburban areas, the car travels around the whole area. Fig. 10 shows a picture of the movable van loaded with CRDS

instrument, and the position of the sampling inlet is about 1.5 m above the ground. Fig. 11 illustrates the route in Hefei and the drive track is colored logarithmically with respect to measured NO_x, NO_2 and NO. The NO_2 concentration ranged from 1.5 ppb to 133.3 ppb and NO ranged from the detection limit to 554.7 ppb. The mean concentrations of NO and NO_2 were 140 ppb and 54.9 ppb, respectively. On the whole, the NO and NO_2 concentrations in urban area were higher than those in suburban area. Large plumes of NO were found at the crossroads with heavy traffic or the sites converged with heavy-duty diesel vehicles. $[NO_2]$ / $[NOx]$ ratio was about 19%, which is larger than the results observed in USA (Wild et al., 2017).

In February 25, 2019 another measurement of vehicle emissions was performed on road to vertify further the instrument performance. NO analyzer (42i), O_3 analyzer (49i) and the CRDS instruments were all placed in a same car. Ambient air was pumped through an inlet fixed on the roof of the car and then divided into three lines to the three instruments, respectively. Fig. 12 illustrates the 4-hour drive track involving highway, urban and suburban area around Hefei, which is colored with respect to the measured NO and NO_2. Vehicle speeds varied greatly on the three different road types and it is around 100 km/h on highway. Influenced by the vehicle emissions, the NOx plumes on urban roads are higher than those on suburban roads and highway.

Fig. 13 shows the time series of NO_2, O_3 and NO. NO_2 concentrations ranged from detection limit to 110.2 ppb and O_3 concentrations ranged from 6.9 ppb to 85.3 ppb. Several NO plumes were observed and the maximum value was up to 767.1 ppb. O_3 and NO showed a significant negative correlation, which is attributed to the quick titration of O_3 by NO. Fig. 14 shows the NO data measured by CRDS and CL analyzer (42i), (a) is the original measurement data and (b) is the data averaged to 1min. The good agreement between the measurement results from the two instruments proves that the CRDS instrument can be applied for fast vehicle NOx emissions.

Because the NO_2 to NOx emissions ratio affects ozone production and spatial distribution, more efforts should be done to provide a constraint on emissions inventories used in air quality modeling. The mobile CRDS instrument provides a good method to retrieve the direct vehicle NOx emission and NO_2 to NOx ratio of plumes due to its easy deployment and high temporal resolution.

5. Conclusion

A compact, sensitive, and accurate instrument based on diode-laser cavity ring-down spectroscopy with the center wavelength of 403.64 nm has been demonstrated for detection of trace amounts of NO_2 and NO_x in ambient air. Minimum detection limits of NO_2 and NO_x were estimated to be 0.030 ppb and 0.040 ppb at an integration time of 1s when zero air is sampled with measurement accuracy of ±5%. Contrast measurement between the dual-channel CRDS instrument and a CL analyzer on NO_2 standard mixtures were performed, which shown a good correlation between the two different techniques. In order to confirm the reliability of the dual-channel CRDS instrument in the field atmosphere, continuous measurement was conducted and the stability of the instrument was investigated. During the intercomparison measurements of NO_2 and NO in the field, the dual-channel CRDS instrument shown a good correlation with the CEAS instrument for NO_2 measurement, and with the CL analyzer for NO measurement.

The CRDS instrument was further deployed in a movable car to monitor NO and NO_2 emission on road. The advantage of high time resolution of the instrument has been demonstrated, which means the instrument provide a new direct method for on-road vehicle plumes measurement. Meanwhile, the high detection sensitivity of the instrument has also shown in this work, which indicates it can act as a new

detection technique for chemistry model verification. It is expected that the instruments developed will
375 lead to the wider application for ambient air quality monitoring and will be useful to investigate
photochemistry in the atmosphere more precisely.

Acknowledgments

This work was supported by National Natural Science Foundation of China (91644107, 61575206,
41571130023 and 61805257) and the National Key Research and Development Program of China
380 (2017YFC0209401, 2017YFC0209403).

References

Ayres, B. R., Allen, H. M., Draper, D. C., Brown, S. S., Wild, R. J., Jimenez, J. L., Day, D. A.,
Campuzano-Jost, P., Hu, W., de Gouw, J., Koss, A., Cohen, R. C., Duffey, K. C., Romer, P., Baumann,
K., Edgerton, E., Takahama, S., Thornton, J. A., Lee, B. H., Lopez-Hilfiker, F. D., Mohr, C.,
385 Wennberg, P. O., Nguyen, T. B., Teng, A., Goldstein, A. H., Olson, K., and Fry, J. L.: Organic nitrate
aerosol formation via NO_3 + biogenic volatile organic compounds in the southeastern United States,
Atmos. Chem. Phys., 15, 13377-13392, doi: 10.5194/acp-15-13377-2015, 2015.

Brent, L. C., Thorn, W. J., Gupta, M., Leen, B., Stehr, J. W., He, H., Arkinson, H. L., Weinheimer, A.,
Garland, C., Pusede, S. E., Wooldridge, P. J., Cohen, R. C., and Dickerson, R. R.: Evaluation of the
390 use of a commercially available cavity ringdown absorption spectrometer for measuring NO_2 in flight,
and observations over the Mid-Atlantic States, during DISCOVER-AQ, J. Atmos. Chem., 72, 503-
521, doi: 10.1007/s10874-013-9265-6, 2013.

Brown, S. S., Dibb, J. E., Stark, H., Aldener, M., Vozella, M., Whitlow, S., Williams, E. J., Lerner, B. M.,
Jakoubek, R., Middlebrook, A. M., DeGouw, J. A., Warneke, C., Goldan, P. D., Kuster, W. C.,
395 Angevine, W. M., Sueper, D. T., Quinn, P. K., Bates, T. S., Meagher, J. F., Fehsenfeld, F. C., and
Ravishankara, A. R.: Nighttime removal of NOx in the summer marine boundary layer, Geophys.
Res. Lett., 31, 1-5, doi: 10.1029/2004gl019412, 2004.

Burgard, D. A., Bishop, G. A., Stadtmuller, R. S., Dalton, T. R., and Stedman, D. H.: Spectroscopy
applied to on-road mobile source emissions, Appl. Spectrosc., 60, 135a-148a, doi:
400 10.1366/000370206777412185, 2006a.

Burgard, D. A., Bishop, G. A., Stedman, D. H., Gessner, V. H., and Daeschlein, C.: Remote sensing of
in-use heavy-duty diesel trucks, Environ. Sci. Technol., 40, 6938-6942, doi: 10.1021/es060989a,
2006b.

Carslaw, D. C., and Beevers, S. D.: Investigating the potential importance of primary NO_2 emissions in
405 a street canyon, Atmos. Environ., 38, 3585-3594, doi: 10.1016/j.atmosenv.2004.03.041, 2004.

Carslaw, D. C.: Evidence of an increasing NO_2/NO_X emissions ratio from road traffic emissions, Atmos.
Environ., 39, 4793-4802, doi: 10.1016/j.atmosenv.2005.06.023, 2005.

Castellanos, P., Luke, W. T., Kelley, P., Stehr, J. W., Ehrman, S. H., and Dickerson, R. R.: Modification
of a commercial cavity ring-down spectroscopy NO_2 detector for enhanced sensitivity, Rev. Sci.
410 Instrum., 80, doi: 10.1063/1.3244090, 2009.

Chen, Y., Yang, C. Q., Zhao, W. X., Fang, B., Xu, X. Z., Gai, Y. B., Lin, X. X., Chen, W. D., and Zhang,
W. J.: Ultra-sensitive measurement of peroxy radicals by chemical amplification broadband cavity-
enhanced spectroscopy, Analyst, 141, 5870-5878, doi: 10.1039/c6an01038e, 2016.

Day, D. A., Wooldridge, P. J., Dillon, M. B., Thornton, J. A., and Cohen, R. C.: A thermal dissociation
415 laser-induced fluorescence instrument for in situ detection of NO_2, peroxy nitrates, alkyl nitrates, and

HNO$_3$, J. Geophys. Res. Atmos., 107, ACH 4-1-ACH 4-14, doi: 10.1029/2001jd000779, 2002.

Duan J., Qin M., Ouyang, B., Fang, W., Li, X., Lu, K. D., Tang, K., Liang, S. X., Meng, F. H., Hu, Z. K., Xie, P.H., Liu, W. Q., Rolf Häsler, Development of an incoherent broadband cavity-enhanced absorption spectrometer for in situ measurements of HONO and NO$_2$. Atmos. Meas. Tech., 11, 4531-4543, doi: 10.5194/amt-11-4531-2018, 2018.

Dunlea, E. J., Herndon, S. C., Nelson, D. D., Volkamer, R. M., San Martini, F., Sheehy, P. M., Zahniser, M. S., Shorter, J. H., Wormhoudt, J. C., Lamb, B. K., Allwine, E. J., Gaffney, J. S., Marley, N. A., Grutter, M., Marquez, C., Blanco, S., Cardenas, B., Retama, A., Villegas, C. R. R., Kolb, C. E., Molina, L. T., and Molina, M. J.: Evaluation of nitrogen dioxide chemiluminescence monitors in a polluted urban environment, Atmos. Chem. Phys., 7, 2691-2704, doi: 10.5194/acp-7-2691-2007, 2007.

Fahey, D. W., Eubank, C. S., Hubler, G., and Fehsenfeld, F. C.: Evaluation of a Catalytic Reduction Technique for the Measurement of Total Reactive Odd-Nitrogen NO$_y$ in the Atmosphere, J.Atmo. Chem., 3, 435-468, doi: 10.1007/bf00053871, 1985.

Fuchs, H., Dube, W. P., Lerner, B. M., Wagner, N. L., Williams, E. J., and Brown, S. S.: A Sensitive and Versatile Detector for Atmospheric NO$_2$ and NOx Based on Blue Diode Laser Cavity Ring-Down Spectroscopy, Environ. Sci. Technol., 43, 7831-7836, doi: 10.1021/es902067h, 2009.

Fuchs, H., Ball, S. M., Bohn, B., Brauers, T., Cohen, R. C., Dorn, H. P., Dube, W. P., Fry, J. L., Haseler, R., Heitmann, U., Jones, R. L., Kleffmann, J., Mentel, T. F., Musgen, P., Rohrer, F., Rollins, A. W., Ruth, A. A., Kiendler-Scharr, A., Schlosser, E., Shillings, A. J. L., Tillmann, R., Varma, R. M., Venables, D. S., Tapia, G. V., Wahner, A., Wegener, R., Wooldridge, P. J., and Brown, S. S.: Intercomparison of measurements of NO$_2$ concentrations in the atmosphere simulation chamber SAPHIR during the NO$_3$Comp campaign, Atmo.Meas.Tech., 3, 21-37, doi: 10.5194/amt-3-21-2010, 2010.

Gherman, T., Venables, D. S., Vaughan, S., Orphal, J., and Ruth, A. A.: Incoherent broadband cavity-enhanced absorption spectroscopy in the near-ultraviolet: Application to HONO and NO$_2$, Environ. Sci. Technol., 42, 890-895, doi: 10.1021/es0716913, 2008.

Herndon, S. C., Shorter, J. H., Zahniser, M. S., Nelson, D. D., Jayne, J., Brown, R. C., Miake-Lye, R. C., Waitz, I., Silva, P., Lanni, T., Demerjian, K., and Kolb, C. E.: NO and NO$_2$ emission ratios measured from in-use commercial aircraft during taxi and takeoff, Environ. Sci. Technol., 38, 6078-6084, doi: 10.1021/es049701c, 2004.

Herndon, S. C., Shorter, J. H., Zahniser, M. S., Wormhoudt, J., Nelson, D. D., Demerjian, K. L., and Kolb, C. E.: Real-time measurements of SO$_2$, H$_2$CO, and CH$_4$ emissions from in-use curbside passenger buses in New York City using a chase vehicle, Environ. Sci. Technol., 39, 7984-7990, doi: 10.1021/es0482942, 2005.

Hueglin, C., Buchmann, B., and Weber, R. O.: Long-term observation of real-world road traffic emission factors on a motorway in Switzerland, Atmos. Environ., 40, 3696-3709, doi: 10.1016/j.atmosenv.2006.03.020, 2006.

Hu, R. Z., Wang, D., Xie, P. H., Chen, H., Ling, L., "Diode Laser Cavity Ring-Down Spectroscopy for Atmospheric NO$_2$ Measurement," Acta. Optica. Sinica. **36**, 0230006, 2016.

Jagerska, J., Jouy, P., Tuzson, B., Looser, H., Mangold, M., Soltic, P., Hugi, A., Bronnimann, R., Faist, J., and Emmenegger, L.: Simultaneous measurement of NO and NO$_2$ by dual-wavelength quantum cascade laser spectroscopy, Opt. Express, 23, 1512-1522, doi: 10.1364/oe.23.001512, 2015.

Jaramillo, P., and Muller, N. Z.: Air pollution emissions and damages from energy production in the US: 2002-2011, Energy Policy, 90, 202-211, doi: 10.1016/j.enpol.2015.12.035, 2016.

460   Karpf, A., Qiao, Y. H., and Rao, G. N.: Ultrasensitive, real-time trace gas detection using a high-power, multimode diode laser and cavity ringdown spectroscopy, Appl. Optics, 55, 4497-4504, doi: 10.1364/ao.55.004497, 2016.

Kasyutich, V. L., Martin, P. A., and Holdsworth, R. J.: Phase-shift off-axis cavity-enhanced absorption detector of nitrogen dioxide, Meas. Sci. Technol., 17, 923-931, doi: 10.1088/0957-0233/17/4/044,
465   2006.

Kebabian, P. L., Wood, E. C., Herndon, S. C., and Freedman, A.: A practical alternative to chemiluminescence-based detection of nitrogen dioxide: Cavity attenuated phase shift spectroscopy, Environ.Sci.Technol., 42, 6040-6045, doi: 10.1021/es703204j, 2008.

Lal, D. R., Clark, I., Shalkow, J., Downey, R. J., Shorter, N. A., Klimstra, D. S., and La Quaglia, M. P.:
470   Primary epithelial lung malignancies in the pediatric population, Pediatr. Blood Cancer, 45, 683-686, doi: 10.1002/pbc.20279, 2005.

Li, Y. Q., Demerjian, K. L., Zahniser, M. S., Nelson, D. D., McManus, J. B., and Herndon, S. C.: Measurement of formaldehyde, nitrogen dioxide, and sulfur dioxide at Whiteface Mountain using a dual tunable diode laser system, J. Geophys. Res. Atmos., 109, 11, doi: 10.1029/2003jd004091, 2004.

475   Li, Z. Y., Hu, R. Z., Xie, P. H., Wang, H.C., Lu, K. D., Wang, D.: Intercomparison of in situ CRDS and CEAS for measurements of atmospheric N_2O_5 in Beijing, China. Science of the Total Environment,613－614 ,131－139. doi: 10.1016/j.scitotenv.2017.08.302, 2018.

Li, Z. Y., Hu, R. Z., Xie, P. H., Chen, H., Wu S. Y., Wang, F. Y., Wang, Y. H., Ling, L. Y., Liu, J. G., and Liu, W. Q.: Development of a portable cavity ring down spectroscopy instrument for simultaneous,
480   in situ measurement of NO_3 and N_2O_5. Optics Express. 26, A433-A449. https://doi.org/10.1364/OE.26.00A433.P, 2018.

Matsumi, Y., Taketani, F., Takahashi, K., Nakayama, T., Kawai, M., and Miyao, Y.: Fluorescence detection of atmospheric nitrogen dioxide using a blue light-emitting diode as an excitation source, Appl. Optics, 49, 3762-3767, doi: 10.1364/ao.49.003762, 2010.

485   Matsumoto, J., Hirokawa, J., Akimoto, H., and Kajii, Y.: Direct measurement of NO_2 in the marine atmosphere by laser-induced fluorescence technique, Atmos. Environ., 35, 2803-2814, doi: 10.1016/s1352-2310(01)00078-4, 2001.

Novikov, S., Lebedeva, N., Satrapinski, A., Walden, J., Davydov, V., and Lebedev, A.: Graphene based sensor for environmental monitoring of NO_2, Sens. Actuator B-Chem., 236, 1054-1060, doi:
490   10.1016/j.snb.2016.05.114, 2016.

Osthoff, H. D., Brown, S. S., Ryerson, T. B., Fortin, T. J., Lerner, B. M., Williams, E. J., Pettersson, A., Baynard, T., Dube, W. P., Ciciora, S. J., and Ravishankara, A. R.: Measurement of atmospheric NO_2 by pulsed cavity ring-down spectroscopy, J. Geophys. Res.-Atmos., 111, doi: 10.1029/2005jd006942, 2006.

495   Osthoff, H. D., Pilling, M. J., Ravishankara, A. R., and Brown, S. S.: Temperature dependence of the NO_3 absorption cross-section above 298 K and determination of the equilibrium constant for $NO_3+NO_2<-> N_2O_5$ at atmospherically relevant conditions, Phys. Chem. Chem.Phys., 9, 5785-5793, doi: 10.1039/b709193a, 2007.

Paul, D., Furgeson, A., and Osthoff, H. D.: Measurements of total peroxy and alkyl nitrate abundances
500   in laboratory-generated gas samples by thermal dissociation cavity ring-down spectroscopy, Rev. Sci. Instrum., 80, doi: 10.1063/1.3258204, 2009.

Platt, U. F., Winer, A. M., Biermann, H. W., Atkinson, R., and Pitts, J. N.: Measurement of nitrate radical concentrations in continental air, Environ. Sci. Tech., 18, 365-369, doi: 10.1021/es00123a015, 1984.

R. McLaren, P. W., D. Majonis, J. McCourt, J. D. Halla, and J. Brook: NO_3 radical measurements in a polluted marine environment:links to ozone formation, Atmo.Chem.Phys., 10, 4187–4206, doi: 10.5194/acp-10-4187-2010, 2010.

Ridley, B. A., and Howlett, L. C.: An instrument for nitric oxide measurements in the stratosphere, Rev. Sci. Instrum., 45, 742-746, doi: 10.1063/1.1686726, 1974.

Sadanaga, Y., Yuba, A., Kawakami, J., Takenaka, N., Yamamoto, M., and Bandow, H.: A gaseous nitric acid analyzer for the remote atmosphere based on the scrubber difference/NO-ozone chemiluminescence method, Anal. Sci., 24, 967-971, doi: 10.2116/analsci.24.967, 2008.

Sadanaga, Y., Suzuki, K., Yoshimoto, T., and Bandow, H.: Direct measurement system of nitrogen dioxide in the atmosphere using a blue light-emitting diode induced fluorescence technique, Rev. Sci. Instrum., 85, 5, doi: 10.1063/1.4879821, 2014.

Sander, S. P., Friedl, R. R., Golden, D. M., Kurylo, M. J., Huie,, R. E., O., V. L., Moortgat, G. K., Ravishankara, A. R.,, and Kolb, C. E., Molina, M. J., and Finlayson-Pitts, B. J.: Chemical Kinetics and Photochemical Data for Use in Atmospheric Studies Evaluation Number 15 Jet Propulsion Laboratory, National Aeronautics and Space Administration/Jet Propulsion Laboratory/ California Institute of Technology, Pasadena, CA, 2006.

Shi, Y. l., Cui, S. h., and Xu, S.,: Factor decomposition of nitrogen oxide emission of China industrial energy consumption, Environ. Sci. Tech., 37, 355-362., 2014.

Sobanski, N., Tang, M. J., Thieser, J., Schuster, G., Pohler, D., Fischer, H., Song, W., Sauvage, C., Williams, J., Fachinger, J., Berkes, F., Hoor, P., Platt, U., Lelieveld, J., and Crowley, J. N.: Chemical and meteorological influences on the lifetime of NO_3 at a semi-rural mountain site during PARADE, Atmos. Chem. Phys., 16, 4867-4883, doi: 10.5194/acp-16-4867-2016, 2016.

Taketani, F., Kawai, M., Takahashi, K., and Matsumi, Y.: Trace detection of atmospheric NO_2 by laser-induced fluorescence using a GaN diode laser and a diode-pumped YAG laser, Appl. Optics, 46, 907-915, doi: 10.1364/ao.46.000907, 2007.

Thieser, J., Schuster, G., Schuladen, J., Phillips, G. J., Reiffs, A., Parchatka, U., Pohler, D., Lelieveld, J., and Crowley, J. N.: A two-channel thermal dissociation cavity ring-down spectrometer for the detection of ambient NO_2, RO_2NO_2 and $RONO_2$, Atmos. Meas. Tech., 9, 553-576, doi: 10.5194/amt-9-553-2016, 2016.

Villena, G., Bejan, I., Kurtenbach, R., Wiesen, P., and Kleffmann, J.: Development of a new Long Path Absorption Photometer (LOPAP) instrument for the sensitive detection of NO_2 in the atmosphere, Atmos. Meas. Tech., 4, 1663-1676, doi: 10.5194/amt-4-1663-2011, 2011.

Villena, G., Bejan, I., Kurtenbach, R., Wiesen, P., and Kleffmann, J.: Interferences of commercial NO_2 instruments in the urban atmosphere and in a smog chamber, Atmos. Meas. Tech., 5, 149-159, doi: 10.5194/amt-5-149-2012, 2012.

Vogt, R., Scheer, V., Casati, R., and Benter, T.: On-road measurement of particle emission in the exhaust plume of a diesel passenger car, Environ. Sci. Tech., 37, 4070-4076, doi: 10.1021/es0300315, 2003.

Voigt, S., Orphal, J., and Burrows, J. P.: The temperature and pressure dependence of the absorption cross-sections of NO_2 in the 250-800 nm region measured by Fourier-transform spectroscopy, J. Photochem. Photobiol., A-Chemistry, 149, 1-7, doi: 10.1016/s1010-6030(01)00650-5, 2002.

Wada, R., and Orr-Ewing, A. J.: Continuous wave cavity ring-down spectroscopy measurement of NO_2 mixing ratios in ambient air, Analyst, 130, 1595-1600, doi: 10.1039/b511115c, 2005.

Wagner, N. L., Dube, W. P., Washenfelder, R. A., Young, C. J., Pollack, I. B., Ryerson, T. B., and Brown, S. S.: Diode laser-based cavity ring-down instrument for NO_3, N_2O_5, NO, NO_2 and O_3 from aircraft,

Atmos. Meas. Tech., 4, 1227-1240, doi: 10.5194/amt-4-1227-2011, 2011.

Wagner, N. L., Riedel, T. P., Young, C. J., Bahreini, R., Brock, C. A., Dube, W. P., Kim, S., Middlebrook, A. M., Ozturk, F., Roberts, J. M., Russo, R., Sive, B., Swarthout, R., Thornton, J. A., VandenBoer, T. C., Zhou, Y., and Brown, S. S.: N_2O_5 uptake coefficients and nocturnal NO_2 removal rates determined from ambient wintertime measurements, J. Geophys. Res.-Atmos., 118, 9331-9350, doi: 10.1002/jgrd.50653, 2013.

Wang, D., Hu, R. Z., Xie, P. H., Liu, J. G., Liu, W. Q., Qin, M., Ling, L.Y., Zeng, Y., Chen, H., Xing, X.B., Zhu, G. L., Wu, J., Duan, J., Lu, X., Shen, L.L., 2015. Diode laser cavity ring-down spectroscopy for in situ measurement of NO_3 radical in ambient air. J. Quant.Spectrosc. Radiat. Transf. 166, 23–29,doi: 10.1016/j.jqsrt.2015.07.005, 2015.

Wang, T., Cheung, V. T. F., Anson, M., and Li, Y. S.: Ozone and related gaseous pollutants in the boundary layer of eastern China: Overview of the recent measurements at a rural site, Geophys. Res. Lett., 28, 2373-2376, doi: 10.1029/2000gl012378, 2001.

Westerdahl, D.: Avoiding Measurement Errors When Monitoring Fine and Ultrafine PM for Exposure and Epidemiology Studies, Epidemiology, 19, S360-S360, 2008.

Wild, R. J., Edwards, P. M., Dube, W. P., Baumann, K., Edgerton, E. S., Quinn, P. K., Roberts, J. M., Rollins, A. W., Veres, P. R., Warneke, C., Williams, E. J., Yuan, B., and Brown, S. S.: A measurement of total reactive nitrogen, NOy, together with NO_2, NO, and O_3 via cavity ring-down spectroscopy, Environ. Sci. Technol., 48, 9609-9615, doi: 10.1021/es501896w, 2014.

Wild, R. J., Dube, W. P., Aikin, K. C., Eilerman, S. J., Neuman, J. A., Peischl, J., Ryerson, T. B., and Brown, S. S.: On-road measurements of vehicle NO_2/NOx emission ratios in Denver, Colorado, USA, Atmos. Environ., 148, 182-189, doi: 10.1016/j.atmosenv.2016.10.039, 2017.

Wu, T., Zhao, W., Chen, W., Zhang, W., and Gao, X.: Incoherent broadband cavity enhanced absorption spectroscopy for in situ measurements of NO_2 with a blue light emitting diode, Appl. Phys. B-Lasers and Optics, 94, 85-94, doi: 10.1007/s00340-008-3308-8, 2009.

Xu, Z., Wang, T., Xue, L. K., Louie, P. K. K., Luk, C. W. Y., Gao, J., Wang, S. L., Chai, F. H., and Wang, W. X.: Evaluating the uncertainties of thermal catalytic conversion in measuring atmospheric nitrogen dioxide at four differently polluted sites in China, Atmos. Environ., 76, 221-226, doi: 10.1016/j.atmosenv.2012.09.043, 2013.

Yamamoto, Y., Sumizawa, H., Yamada, H., and Tonokura, K.: Real-time measurement of nitrogen dioxide in vehicle exhaust gas by mid-infrared cavity ring-down spectroscopy, Appl. Phys. B, 105, 923-931, doi: 10.1007/s00340-011-4647-4, 2011.

Yang, W., and Omaye, S. T.: Air pollutants, oxidative stress and human health, Mutat. Res. Genet. Toxicol. Environ. Mutagen., 674, 45-54, doi: 10.1016/j.mrgentox.2008.10.005, 2009.

Yuba, A., Sadanaga, Y., Takami, A., Hatakeyama, S., Takenaka, N., and Bandow, H.: Measurement System for Particulate Nitrate Based on the Scrubber Difference NO-O_3 Chemiluminescence Method in Remote Areas, Anal. chem., 82, 8916-8921, doi: 10.1021/ac101704w, 2010.

Table 1 Comparison of NO$_2$ detection limits based on optical methods.

Principle of measurement	Laser power	Wavelength range/nm	Dectection limit	Reference
Cw-CRDS	5mW(1MHz)	410	80ppt/50s(1σ)	(Wada and Orr-Ewing, 2005)
ND:YAG laser CRDS	1mJ	532	40ppt/1s(1σ)	(Osthoff et al., 2006)
pDL-CRDS	40 mW(2KHz-10%)	404	11ppt/1s(1σ)	(Fuchs et al., 2009)
Fabry-Perot (FP) pDL-CRDS	1.1w (4KHZ-10%)	400	38ppt/128ms(1σ)	(Karpf et al., 2016)
commercial DL-CRDS	1.2KHZ	407.38	20ppt/60s(1σ)	(Castellanos et al., 2009)
LED-based commercial CRD	355 mW	397-412(405)	27ppt/60s(1σ)	(Brent et al., 2013)
LED-CEAS	340mw	455	2.2ppb/100s(1σ)	(Wu et al., 2009)
Xe lamp DOAS		295–492 nm	1ppb/480s(1σ)	(R. McLaren, 2010)
CAPS		440	20ppt/10s(1σ)	(Kebabian et al., 2008)
diode-pumped Nd:YAG laser-LIF	15mw(14KHz)	473	70/60s(1σ)	(Taketani et al., 2007)
blue LED-IF	17.7mw(10KHz)	435	4.9ppb/60s(1σ)	(Matsumi et al., 2010)
pulsed blue light LED-LIF	22mw	430	3.5ppb/60s(1σ)	(Sadanaga et al., 2014)
pDL-CRDS	60mw	403.64	30ppt/1s(1σ)	This work

CRDS=cavity ring-down spectroscopy; CEAS=cavity-enhanced absorption spectroscopy; BB=broadband; DOAS=differential optical absorption spectroscopy; cw=continuous-wave diode laser. LIF=laser induced fluorescence; CAPS= cavity attenuated phase shift spectroscopy; pDL=pulsed diode laser.

590
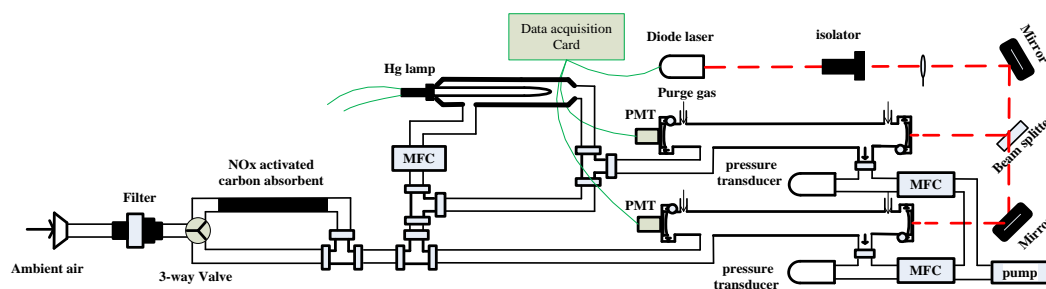
Fig. 1. Schematic of the dual-channel Cavity Ring down Spectroscopy system.
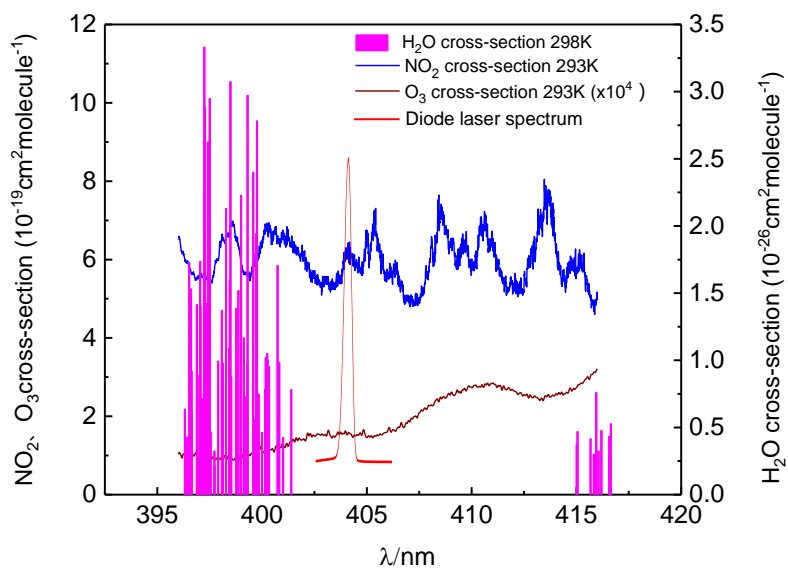
Fig. 2. Cross section of the NO$_3$ radical, NO$_2$, O$_3$, water vapor, and diode laser spectrum.

595
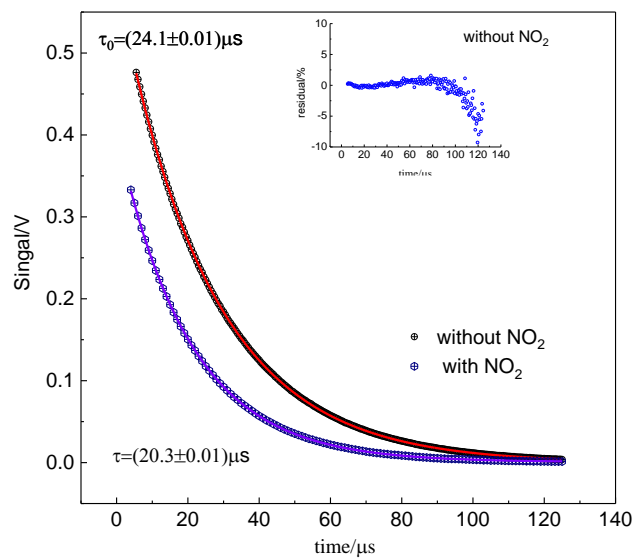
Fig. 3. Different cavity ring-down signals and fitting results in the absence and presence of NO$_2$. The small figure in the upper right corner is the fitting residual.

600
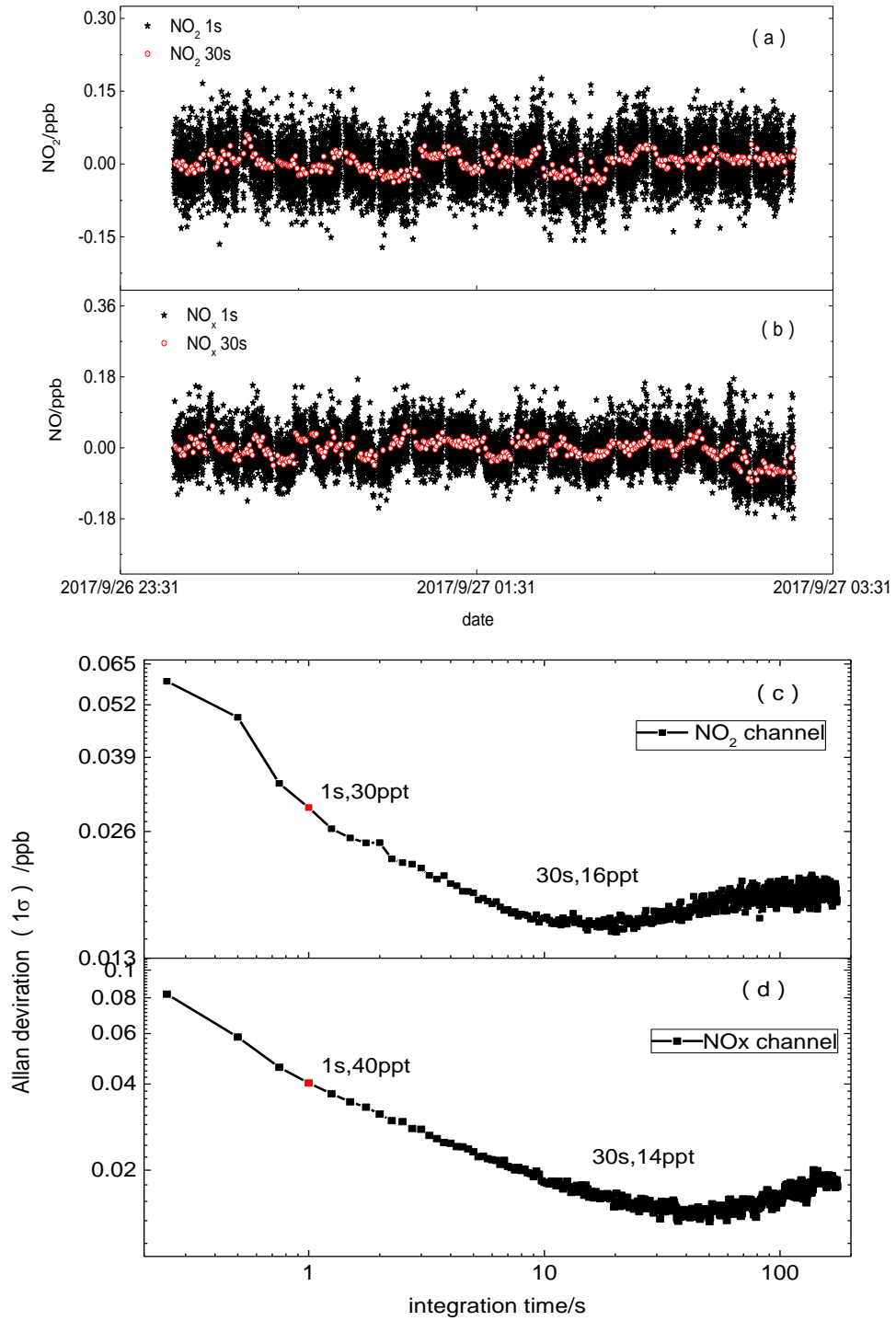
Fig. 4. (a) (b) Continuous time series measurement when the instrument sampled only zero air, averaged to 1s for NO$_2$ and NO$_x$ channels (black dots), the red dots show the data averaged to 30s, (c) (d): Allan deviation plots for NO$_2$ concentration in two channels. The minimum value equals the optimum integration time.
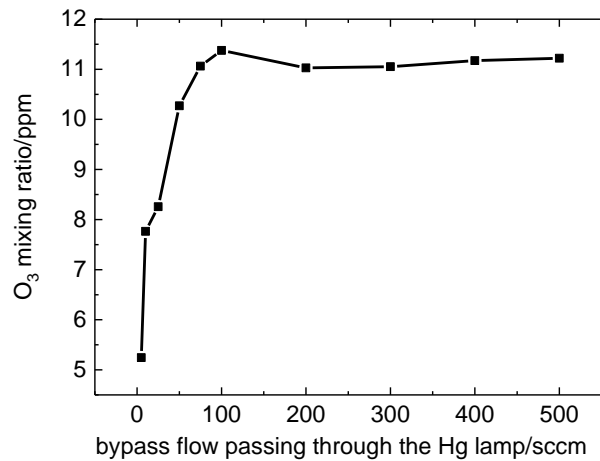
Fig. 5. O$_3$ mixing ratio when changing the bypass flow passing through Hg lamp.
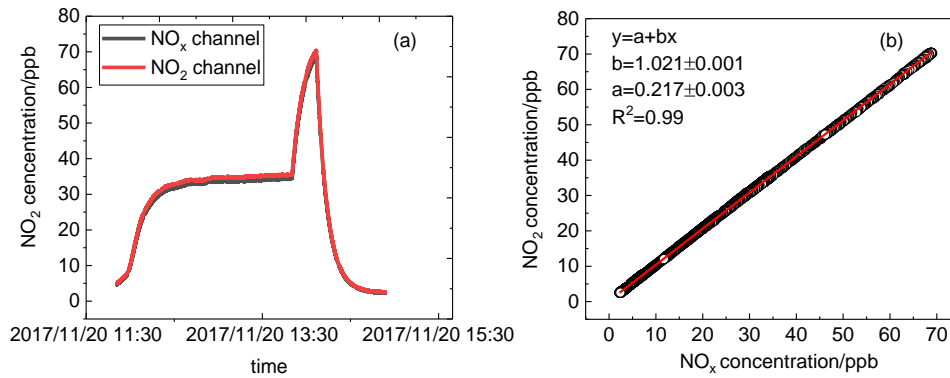
Fig. 6. (a) Time series of NO$_2$ concentration sampled standard mixtures by CRDS instrument in two

 channels with mercury pen-ray lamp switched on. (b) A correlation plot between the data from two

channels.
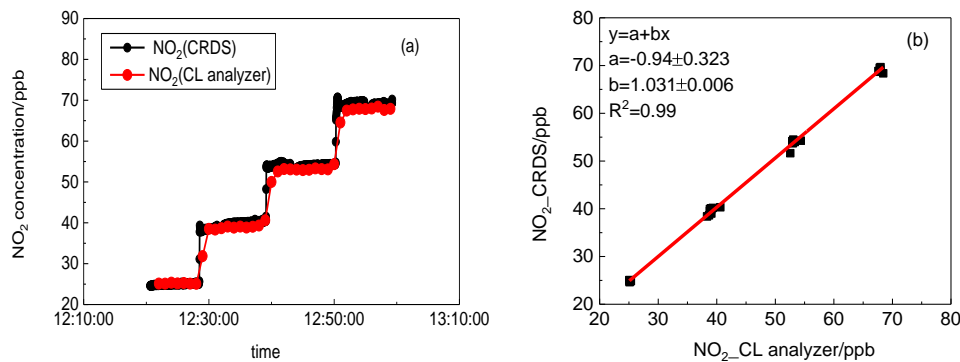
Fig. 7. (a) Time series of NO$_2$ concentration sampled standard mixtures by CRDS instrument and CL

 analyzer. The time resolution for CRDS instrument and CL analyzer are 1s and 1min, respectively. (b) A

correlation plot between the data from the CRDS instrument and the CL analyzer (data averaged to

1min). The fitting result gave a gradient of 1.031 and an intercept of -0.940 ppb, with linear correlation

factor of 0.99.
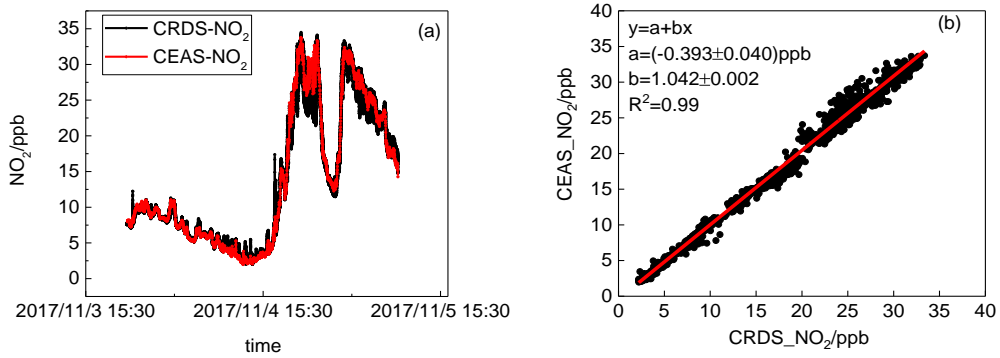
Fig. 8. (a) NO$_2$ mixing ratios by CEAS (1 min average) and CRDS (1 s average) instruments, (b) Scatter plots for the NO$_2$ dataset from CRDS and CEAS instrument. The red lines illustrate the linear regression (Data averaged to 1 min base).
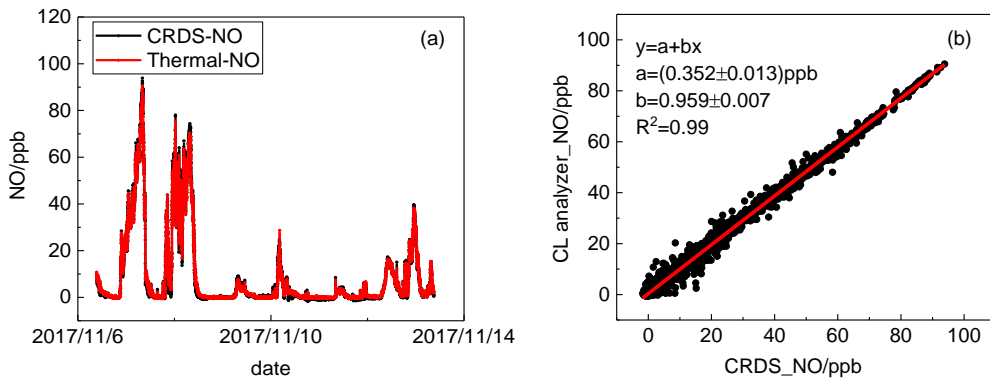
Fig. 9. (a) Time series of NO by dual-CRDS instrument and CL analyzer. (b)A correlation between two instruments is shown and data for correlation analysis is averaged in 1min.
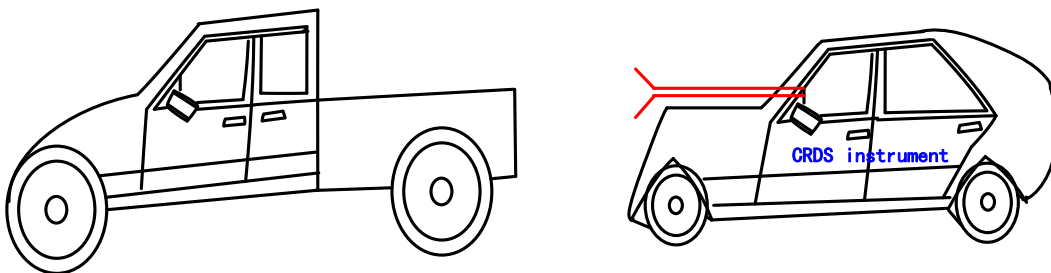
Fig. 10. The diagram of the movable van loaded with CRDS instrument.
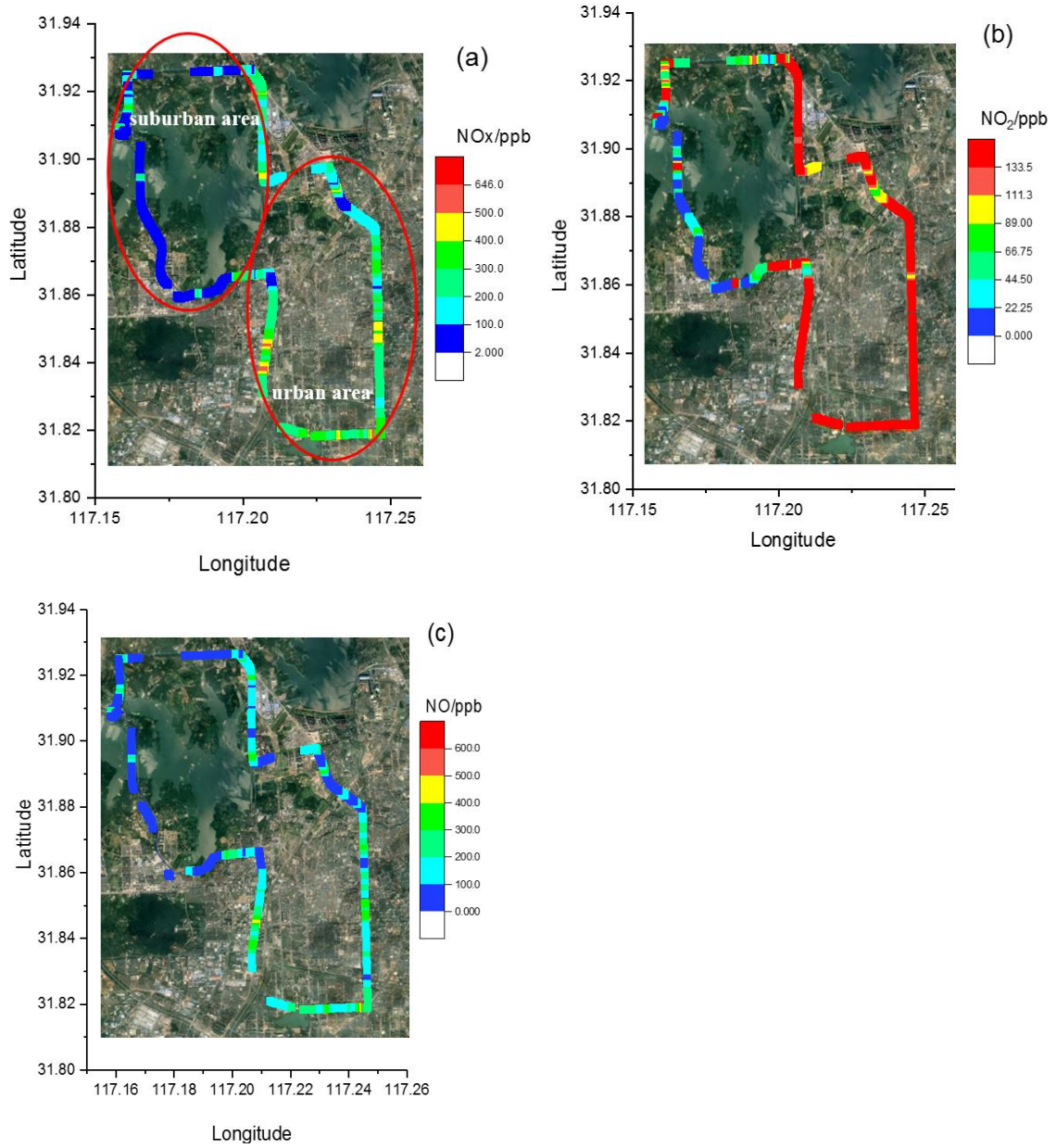
Fig. 11. Results of the NOx (a), NO$_2$ (b) and NO (c) concentrations around Hefei, China (Data is averaged to 5 s).
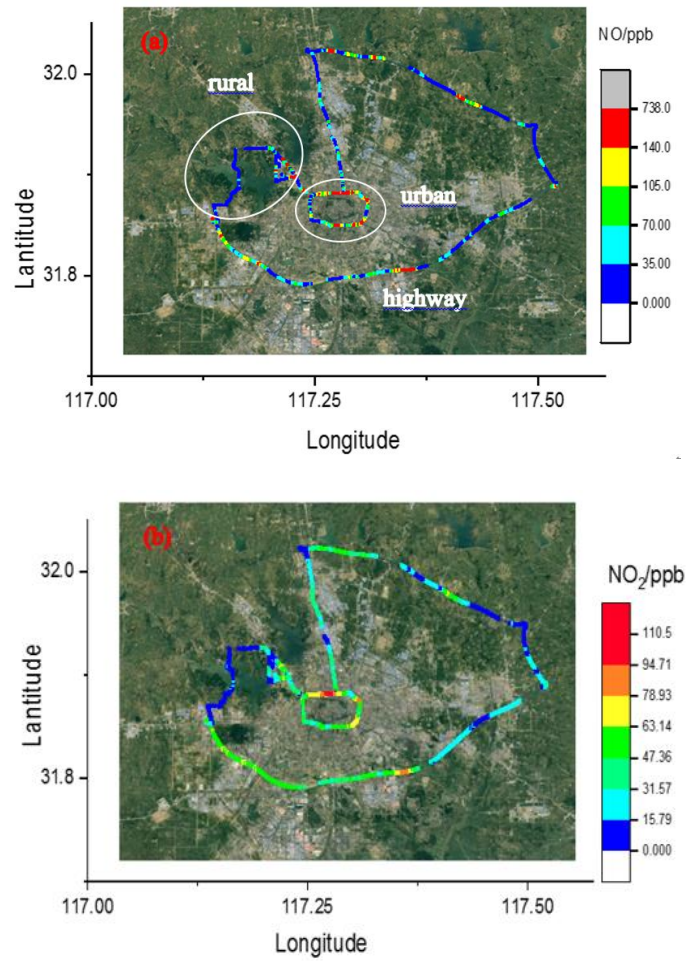
635

Fig.12.The 4-h drive around Hefei, China, colored by the measured NO (a) and NO$_2$ (b) concentrations, respectively.
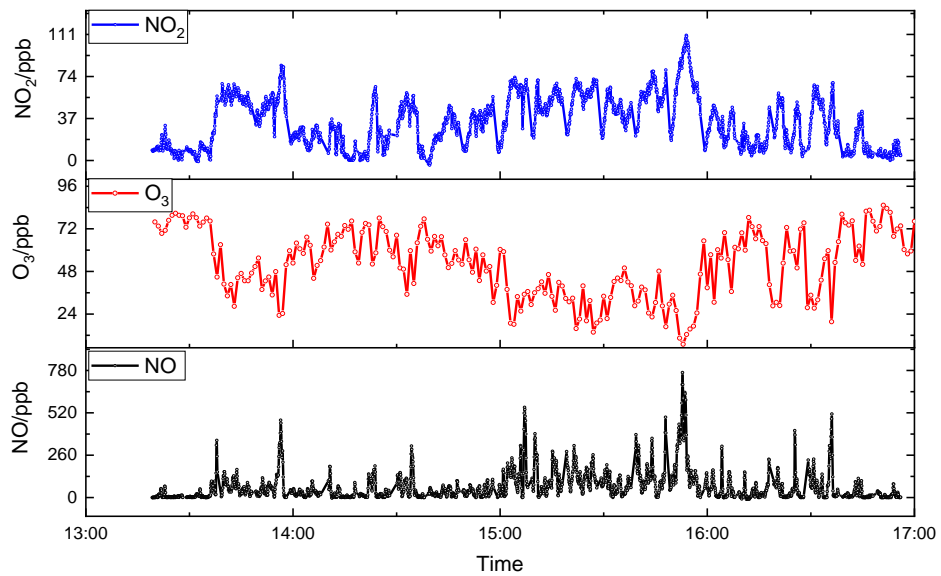
Fig.13. Results of the NO$_2$, NO and O$_3$ concentrations around Hefei, China.
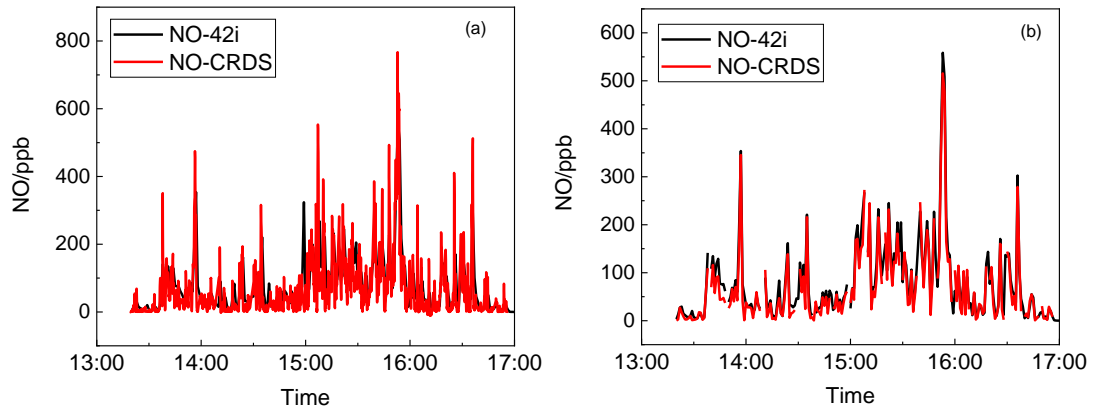
640   Fig.14. Time series of NO by CRDS instrument and CL analyzer (42i). (a) is the original measurement

data and (b) is the data averaged to 1min.